TRENDS IN SCIENCES 2026; 23(4): 11542
https://doi.org/10.48048/tis.2026.11542 RESEARCH ARTICLE

Targeting Inflammatory Pathways via Molecular Docking and *In vivo* Assessment of *Prunus amygdalus* Stem Bark-Derived Flavonoids and Rutin

Dilovar Karimova[1,*], Xilola Burxanova[1], Izzatullo Khikmatullaev[1] and Nargiza Azimova[2]

[1]*Kokand State University, Dept of Chemistry, Fergana, Uzbekistan*
[2]*Pedagogical Skill Center of Fergana Region, Fergana, Uzbekistan*

([*]Corresponding author's e-mail: karimova_bd@mail.ru)

Received: 8 August 2025, Revised: 5 September 2025, Accepted: 25 October 2025, Published: 25 December 2025

Abstract

Almond (*Prunus amygdalus*) steam bark, an agro-industrial by-product rich in polyphenolic compounds, represents a sustainable source of bioactive flavonoids, particularly rutin, with potential pharmacological applications. In this study, total flavonoids were extracted using ethanol-based maceration combined with ultrasonic treatment and vacuum concentration, yielding a high-purity fraction (98.0 ± 0.8%), while rutin was isolated through semi-preparative HPLC. Acute oral toxicity assessment in male mice at a limit dose of 5,000 mg/kg revealed no mortality, no significant changes in body weight ($p > 0.05$), and only mild transient behavioral alterations, indicating an $LD_{50} > 5{,}000$ mg/kg and classification under GHS Category 5 (low toxicity). In the carrageenan-induced paw edema model, the flavonoid fraction at 100 mg/kg and rutin at 25 mg/kg exhibited the highest anti-inflammatory activity, with 61.6% and 55.6% inhibition of edema formation at the third hour, respectively, while higher doses showed moderate but sustained effects, suggesting a non-linear dose-response relationship. Molecular docking studies demonstrated strong binding affinities of rutin to inflammation-related protein targets, including TNF-α (–7.8 kcal/mol, Ki = 1.92 µM), AKT1 (–8.8 kcal/mol, Ki = 0.36 µM), and ESR1 (–8.5 kcal/mol, Ki = 0.61 µM), as well as high-affinity binding to serum albumin (–10.4 kcal/mol, Ki = 23.2 nM). These findings indicate that almond steam bark-derived flavonoids and rutin are safe at high oral doses, exert potent anti-inflammatory effects, and act via multi-target modulation of inflammatory pathways, supporting their potential as natural therapeutic or nutraceutical agents.

Keywords: *Prunus amygdalus*, Almond bark, Flavonoids, Rutin, Anti-inflammatory, Molecular docking, Carrageenan-induced paw edema, Acute toxicity

Introduction

Prunus dulcis (Mill.) D.A. Webb - the almond tree - is one of the most widely cultivated and economically important nut crops in the world. Its kernels are widely used in the food industry as a valuable source of oil, proteins, minerals, and vitamins. However, during almond processing, a large amount of by-products such as stem bark, skin, shell, and leaves are generated. While these parts are often considered agricultural waste, they are increasingly recognized as potential sources of bioactive compounds of nutraceutical and pharmaceutical value [1].

The stem bark of Prunus dulcis remains poorly studied compared with the kernel, skin, or shell, yet it represents a promising raw material rich in phenolic compounds, flavonoids, tannins, and phenolic acids. In particular, rutin and quercetin glycosides are believed to be abundant in almond bark, conferring strong antioxidant and anti-inflammatory properties. Previous studies have mainly focused on almond skin and shell. For example, Garrido *et al.* [1] analyzed the phenolic profile of almond skins and identified 33 types of flavonoids and glycosides, confirming their strong antioxidant potential. Similarly, Smeriglio *et al.* [2]

investigated shell extracts by HPLC-DAD and reported both antioxidant and antidiabetic properties [3].

In contrast, systematic phytochemical and pharmacological studies of almond bark are very limited. This creates a scientific gap and highlights the need for new investigations. As suggested by Ahmed *et al.* [3], almond by-products, often regarded as waste, may serve as sustainable sources of high-value nutraceuticals [4].

Recent studies confirm that extracts from different parts of Prunus dulcis exhibit remarkable antioxidant and anti-inflammatory activities. Ali *et al.* [5] demonstrated that seed fractions displayed strong radical scavenging properties in DPPH and FRAP assays. Furthermore, Yada *et al.* [6] reviewed the composition and health benefits of almonds, emphasizing their preventive role against cancer, cardiovascular, and metabolic disorders [6].

The significance of almond stem bark lies in its dual value: despite being an agricultural by-product, it is potentially rich in high-value bioactive compounds. Efficient extraction and utilization of such compounds could transform waste into a resource, adding economic value and sustainability. Particularly, rutin isolation and its mechanistic evaluation through in vivo anti-inflammatory testing and in silico molecular docking provide a scientific foundation for the development of novel natural therapeutics [7,8].

Therefore, the present study aims to extract total flavonoids and isolate rutin from Prunus dulcis stem bark, assess their safety profile through acute oral toxicity (LD_{50}), evaluate their anti-inflammatory potential using the carrageenan-induced paw edema model, and investigate their molecular interactions with key inflammation-related proteins through docking simulations. This integrated approach will provide valuable insights into the pharmacological potential of almond stem bark, supporting its future application in nutraceuticals and functional food formulations [9,10].

Materials and methods

Animal ethics

All preoperative and experimental protocols were read and approved slowly by the Institutional Committee for Animal Use and Care. The animals lived in vivarium rooms under controlled conditions, relative humidity of 55% - 65%, ambient temperature of 22 ± 2 °C, and had free access to water and normal laboratory chow. All animal handling and care procedures rigorously followed the European Directive 2010/63/EU on the protection of animals used for scientific purposes. Ethical approval for this research was provided by the Institute of Bioorganic Chemistry, Academy of Sciences of the Republic of Uzbekistan, Animal Ethics Committee (Protocol No. 133/1a/h, 4 August 2014).

Plant material and preparation

Fresh stem bark of *Prunus dulcis* (Mill.) D.A. Webb was collected from 8 - 10-year-old cultivated almond trees in the Fergana region, Uzbekistan, during the harvesting season (May - June). The plant material was taxonomically identified and authenticated at the Department of Botany, Fergana State University. The bark was washed with distilled water, air-dried at 25 ± 2 °C to a constant weight, and ground into a fine powder. For flavonoid extraction, the material was sieved to a particle size of 0.5 mm, while for rutin isolation, a particle size of 0.1 - 1.5 mm was used. The powdered samples were stored in airtight containers at 4 °C until analysis [11].

Chemicals and reagents

All solvents and reagents were of analytical or HPLC grade. Ethanol (≥ 99%), acetonitrile, and buffer salts were obtained from Sigma-Aldrich (St. Louis, MO, USA). Distilled water was prepared using a Milli-Q purification system (Millipore, USA). All other chemicals were purchased from local suppliers and used without further purification.

Extraction of total flavonoids

Fifty g of powdered almond bark (0.5 mm particle size) was extracted with 250 mL of 70% ethanol at 50 - 60 °C for 2 h under continuous stirring in a flat-bottom flask equipped with a reflux condenser. The extract was subjected to ultrasonic treatment for 15 min (2 cycles, 10 min interval) at 35 °C and filtered through ashless filter paper (blue ribbon). The residue was re-extracted with an additional 250 mL of 70% ethanol under identical conditions for 1.5 h, followed by ultrasonic treatment for 10 min (2 cycles, 8 min interval) at 35 °C. The combined extracts were supplemented with a 20 mL distilled water rinse of the plant residue. The organic

solvent was removed by vacuum evaporation (10 - 30 mm Hg) in a rotary evaporator, and the aqueous fraction was lyophilized to yield the total flavonoid fraction [12].

Semi-preparative isolation and purification of rutin

Ten g of powdered almond steam bark (0.1 - 1.5 mm) was extracted with 99 mL of 70% ethanol at 50 - 60 °C for 2 h under continuous stirring in a reflux-equipped flat-bottom flask [13]. The extract underwent ultrasonic treatment for 15 min (2 cycles, 10 min interval) at 35 °C and was cooled to room temperature. The filtrate was passed through ashless filter paper followed by a 0.2 µm membrane filter. Rutin was separated using an Agilent Technologies 1260 HPLC system with a semi-preparative XBridge® BEH C18 column (130 Å, 5 µm, 10×250 mm^2; Waters). The mobile phase consisted of acetonitrile and buffer (30:70, pH 2.92) under isocratic elution at 2.00 mL/min, with a total runtime of 15 min. Detection was performed at 254 nm using a diode-array detector (DAD). Rutin was collected in the retention time range of 2.2 - 2.4 min over 15 automated injections. The organic fraction was evaporated under reduced pressure, and the aqueous fraction was lyophilized [14].

Acute oral toxicity study

Acute toxicity was assessed according to the OECD Guideline 423 (Acute Toxic Class Method). Mice were randomly divided into 3 groups (n = 5 per group): Control, flavonoid fraction (5,000 mg/kg), and rutin (5,000 mg/kg). Test substances were administered orally as a single dose via gavage [15]. Animals were observed continuously for 4 h post-dosing and periodically over 14 days for signs of toxicity, behavioral changes, and mortality. Body weight was recorded on days 0, 7, and 14. Gross necropsy was performed at the end of the observation period [16].

Anti-inflammatory activity: Carrageenan-induced paw edema model

Anti-inflammatory activity was evaluated using the carrageenan-induced paw edema model in mice. Animals were divided into treatment and control groups (n = 5). The flavonoid fraction was administered at doses of 100, 150, and 200 mg/kg, and rutin at 25, 50, and 75 mg/kg, 1 h before carrageenan injection. Edema was induced by subplantar injection of 0.1 mL of 1% carrageenan suspension in saline into the right hind paw [17,18]. The control group received saline only and carrageenan. Paw volume was measured before and at hourly intervals for 5 h after carrageenan injection using a plethysmometer. Edema inhibition (%) was calculated relative to the control group [19].

Molecular docking studies

The 3D structures of TNF-α (PDB ID: 2AZ5), AKT1 (PDB ID: 7NH5), BCL2 (PDB ID: 6GL8), serum albumin (PDB ID: 6R7S), and ESR1 (PDB ID: 1L2I) were retrieved from the Protein Data Bank. The structure of rutin was obtained from the PubChem database. All docking studies were performed using AutoDock 4.2.6, with proteins prepared by removing water molecules and adding polar hydrogens [20,21]. The grid box dimensions were set to cover the active site coordinates for each protein. Docking results were analyzed using AutoDock Tools and Discovery Studio Visualizer, and key ligand–protein interactions recorded [22].

Statistics

Statistical evaluation and graphical representations were performed using Origin Pro 9 software (Microsoft, USA). Paired t-tests were used for analyzing combined data sets, while unpaired t-tests assessed differences between separate groups. Results were considered statistically significant at the threshold of $p < 0.05$.

Results

Extraction and isolation of flavonoid and rutin compounds from almond steam bark

Extraction of total flavonoids

The plant raw material was ground to a particle size of approximately 0.5 mm. A 50 g portion was extracted with 250 mL of 70% ethanol at 50 - 60 °C for 2 h under continuous stirring in a flat-bottom flask equipped with a reflux condenser [23]. The resulting extract was subjected to ultrasonic treatment for 15 min (2 cycles of 10 min intervals) at 35 °C. The extract was filtered through ashless filter paper (blue ribbon). The residue was re-extracted with an additional 250 mL of 70% ethanol under the same conditions for 1.5 h, followed by ultrasonic treatment for 10 min (2 cycles, 8

min interval) at 35 °C. After filtration, both extracts were combined, and the remaining plant residue was rinsed with 20 mL of distilled water, which was also added to the combined extracts. The organic solvent was removed by vacuum evaporation (10 - 30 mm Hg) using a rotary evaporator [24]. The aqueous fraction containing the total flavonoids was lyophilized. This procedure yielded a total flavonoid fraction with a purity of 98.0 ± 0.8%.

Semi-preparative isolation and purification of rutin

Dried vegetative parts of the plant were milled to a particle size of 0.1 - 1.5 mm. A 10 g sample was extracted with 99 mL of 70% ethanol at 50 - 60 °C for 2 h under continuous stirring in a flat-bottom flask with a reflux condenser [25]. The extract underwent ultrasonic treatment for 15 min (2 cycles of 10 min intervals) at 35 °C, then cooled to room temperature. The solution was first filtered through ashless filter paper (blue ribbon), followed by membrane filtration (0.2 µm).

High-performance liquid chromatography (HPLC) analysis was performed under isocratic conditions with a diode-array detector (DAD) using an Agilent Technologies 1260 system. The mobile phase consisted of acetonitrile and buffer (30:70, pH 2.92), with a flow rate of 2.00 mL/min, injection volume 50 µL, and total analysis time of 15 min. A semi-preparative XBridge® BEH C18 column (130 Å, 5 µm, 10×250 mm^2, Waters) was used, with detection at 254 nm. Rutin was collected in the retention time range of 2.2 - 2.4 min over 15 automated injections. The organic fraction was evaporated under reduced pressure, and the aqueous fraction was lyophilized to obtain purified rutin.

Figure 1 Bark of almond (*Prunus amygdalus*).

Acute oral toxicity evaluation of almond steam bark-derived flavonoid and rutin in male mice

To evaluate the acute toxicity profile of the flavonoid and rutin compounds isolated from almond (*Prunus amygdalus*) Bark, an oral administration study was conducted in male mice following the OECD Guideline 423 for acute toxic class method [26,27]. Both compounds were administered as a single high dose of 5,000 mg/kg body weight, which is considered the upper limit dose for identifying toxic potential. Following administration of the flavonoid fraction at 5,000 mg/kg, animals exhibited mild, transient clinical signs within 10 min (**Figure 1**). These included increased respiratory rate, grouping behavior (animals huddled together), and narrowed palpebral fissures (partially closed eyes).

Table 1 Evaluation parameters of acute toxicity of flavonoid and rutin compounds isolated from almond steam bark in male mice (M ± m, n = 5).

Groups	Doses mg/kg, mL	Total animals / Died animals	Average weight of animals(g)			LD_{50}, mg/kg
			Day 1	Day 7	Day 14	
Control	0.4 mL	5/0	22.0 ± 1.9	22.6 ± 2.2	23.2 ± 2.3	-
Almond steam bark flavonoid	5,000 mg/kg	5/0	21.6 ± 1.8	21.9 ± 2.1	23.0 ± 2.2	> 5,000
Almond steam bark rutin	5,000 mg/kg	5/0	21.0 ± 2.0	21.7± 2.0	22.8 ± 2.1	> 5,000

These signs persisted for approximately 20 to 30 min, after which the animals gradually returned to normal behavior and showed no further abnormalities for the remainder of the 14-day observation period. Similarly, administration of the rutin compound at the same dose resulted in observable changes approximately 15 min post-dosing. Treated animals exhibited mild respiratory stimulation and immobility in a fixed location. These signs were transient and resolved spontaneously within 25 to 40 min, with full recovery to baseline behavior and physiological status. Importantly, no mortality was recorded in either test group throughout the observation period (0 deaths out of 5 animals per group). Body weight was monitored on days 1, 7, and 14 to detect any potential systemic toxicity. The test groups (flavonoid and rutin) showed no statistically significant deviation in mean body weight compared to the control group at any time point ($p > 0.05$), indicating the absence of weight loss or growth retardation associated with the administered compounds. Mean body weights remained stable or increased slightly over the 14-day period, suggesting good systemic tolerance (**Figure 2**). Gross observations during the study did not reveal any signs of gastrointestinal distress, tremors, convulsions, or other toxicological markers [28,29]. Based on the absence of mortality and minimal, short-term behavioral symptoms that resolved without intervention, the median lethal dose (LD_{50}) for both the almond steam bark-derived flavonoid and rutin compounds was estimated to be greater than 5000 mg/kg. These findings demonstrate that both compounds, when administered orally as a single high dose, exhibit low acute toxicity in male mice. According to the Globally Harmonized System (GHS) for classification of chemical substances, compounds with LD_{50} values exceeding 5000 mg/kg fall under Category 5 (or unclassified), indicating a very low level of toxicity.

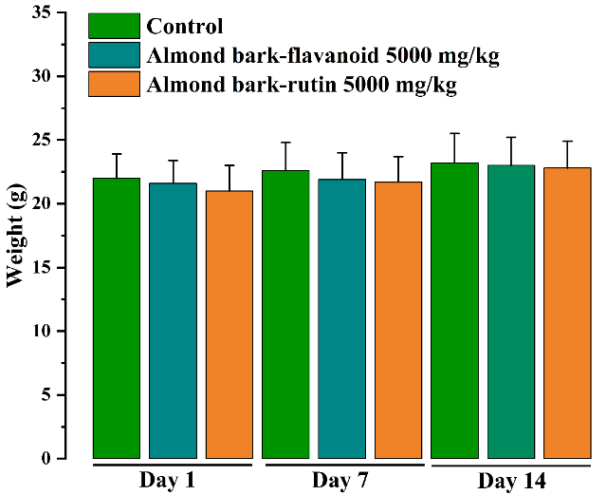

Figure 2 Effect of oral administration of almond steam bark-derived flavonoid and rutin (5,000 mg/kg) on body weight in male mice over 14 days.

Overall, the results confirm the safety of oral administration of almond steam bark-derived flavonoid and rutin at high doses, supporting their potential use as bioactive compounds in pharmacological formulations, functional foods, or nutraceuticals. Further subacute and chronic toxicity studies are recommended to fully assess long-term safety profiles, including organ-specific histopathology and biochemical parameters.

Anti-inflammatory activity of flavonoid and rutin compounds isolated from almond steam bark in the carrageenan-induced paw edema model

To experimentally verify the predicted anti-inflammatory potential of flavonoid and rutin compounds isolated from *Prunus amygdalus* (almond) steam bark, we employed the well-established carrageenan-induced paw edema model in rodents. This model closely mimics the acute inflammatory response in vivo and allows for quantification of both early and late phases of inflammation [30]. Upon carrageenan injection into the plantar surface of the hind paw, local inflammation is initiated through the rapid release of histamine and serotonin (early phase, 0 - 2 h), followed by a delayed phase dominated by prostaglandins, bradykinin, nitric oxide, and pro-inflammatory cytokines such as IL-1β, TNF-α, and IL-6 (2 - 5 h). This biphasic mechanism enables the evaluation of test compounds' effects on both vascular and cellular components of inflammation (**Table 1**).

In this study, experimental animals were divided into several groups, each receiving different doses of the isolated flavonoid extract (100, 150 and 200 mg/kg) or rutin (25, 50 and 75 mg/kg) prior to the administration of carrageenan. The control group received saline and carrageenan but no treatment. Paw volume was measured hourly over a 5-hour period using plethysmometric analysis (**Figure 3**). The degree of edema was calculated and expressed as percentage inhibition of inflammation relative to the control group, providing a direct comparison of anti-inflammatory efficacy [31].

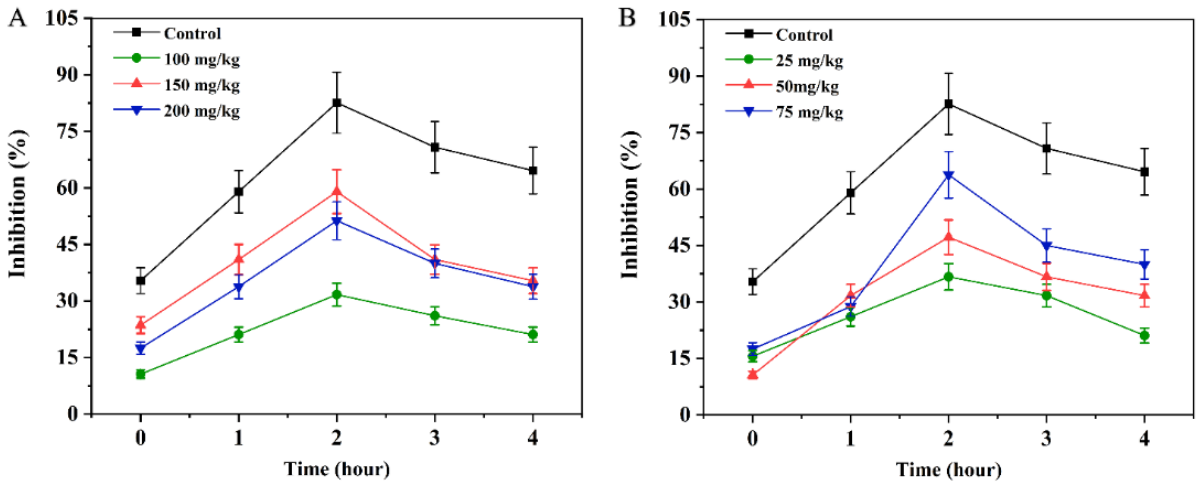

Figure 3 Time-dependent anti-inflammatory effects of flavonoid and rutin compounds isolated from almond steam bark in the carrageenan-induced paw edema model. (A) Inhibitory effect of flavonoid extract at doses of 100, 150, and 200 mg/kg compared to the control group over a 4-hour period following carrageenan injection. (B) Inhibitory effect of rutin at doses of 25, 50, and 75 mg/kg compared to the control group over the same time period.

The control group exhibited the highest edema response, with a mean paw swelling of 82.6 ± 8.1% at the 3rd h post-carrageenan injection - coinciding with the peak of the exudative phase. This time point was therefore selected as the standard for calculating anti-exudative efficacy across groups [32].

Among all tested doses, the flavonoid extract at 100 mg/kg exhibited the most prominent anti-exudative effect, achieving 61.6% inhibition of edema formation. This was followed closely by rutin at 25 mg/kg, which yielded 55.6% inhibition. Higher doses of flavonoid (150 and 200 mg/kg) and rutin (50 and 75 mg/kg) showed moderate but consistent anti-inflammatory

responses ranging from 22.8% to 42.9%, indicating a non-linear dose-response relationship. This suggests that lower doses may be more bioavailable or interact more effectively with relevant inflammatory targets, potentially due to solubility, pharmacokinetics, or receptor saturation dynamics (**Figure 4**).

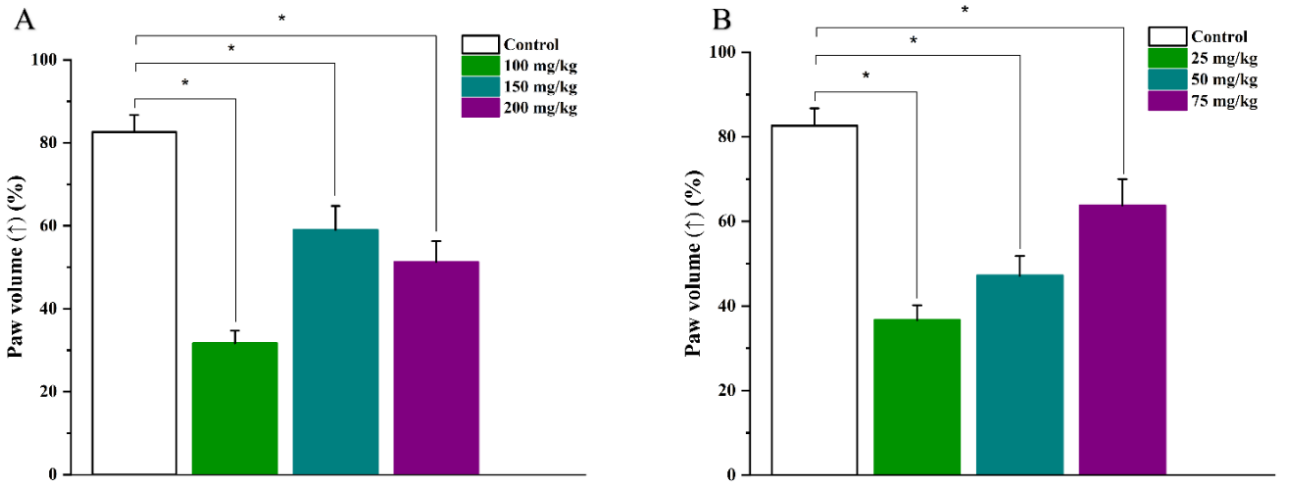

Figure 4 Effect of flavonoid and rutin compounds isolated from almond steam bark on carrageenan-induced paw edema in rats. (A) Flavonoid extract significantly reduced paw volume at doses of 100, 150, and 200 mg/kg compared to the control group. (B) Rutin also inhibited paw edema volume at doses of 25, 50, and 75 mg/kg, with the strongest effect observed at 25 mg/kg. Paw edema volume (%) was measured at 3 h post-carrageenan injection - the peak of the inflammatory response. Values are expressed as mean ± SEM (n = 5). Asterisks (*) indicate statistically significant differences compared to the control group (*$p < 0.05$).

Time-course analysis of edema inhibition revealed that all treated groups demonstrated the strongest anti-inflammatory response at the 3rd h post-carrageenan injection. This observation aligns with the established peak of prostaglandin-mediated inflammation, supporting the hypothesis that the tested compounds may exert their effects via modulation of COX enzymes, cytokine release, or leukocyte recruitment. Notably, rutin at 75 mg/kg produced 63.8 ± 6.2% inhibition at this time point, closely matching the efficacy of the flavonoid 100 mg/kg group. The flavonoid extract at 150 mg/kg showed 59.0 ± 5.8%, and rutin at 50 mg/kg achieved 47.2 ± 4.6% inhibition, respectively. These results suggest comparable or even synergistic potential between the flavonoid fraction and rutin in modulating acute inflammatory responses [33].

At the 4th and 5th h, a gradual decline in anti-inflammatory activity was observed in most treatment groups. This pattern may be attributed to metabolic breakdown, hepatic clearance, or redistribution of the compounds within the body. Nevertheless, inhibition remained statistically significant compared to control even at later time points, confirming that the compounds have sustained, though time-limited, anti-inflammatory effects.

The underlying mechanisms of these effects are likely multifactorial. Based on earlier molecular docking studies, both flavonoids and rutin demonstrated strong binding affinities to key inflammation-related proteins, including TNF-α, COX-2, AKT1, and ESR1. These in silico predictions provide a plausible molecular basis for the observed in vivo efficacy, suggesting that the compounds may downregulate inflammatory pathways at the transcriptional or post-translational level. Furthermore, flavonoids and rutin are known for their antioxidant properties, which may further contribute to the stabilization of endothelial cells, reduction of vascular permeability, and scavenging of reactive oxygen species generated during inflammation [34].

Table 1 Original paw images of carrageenan-induced inflammation in rats used to assess the anti-inflammatory effects of almond steam bark-derived flavonoid and rutin compounds.

Inhibiting inflammation 3-hour images	
	
Control	Almond steam bark-Flavanoid 100 mg/kg
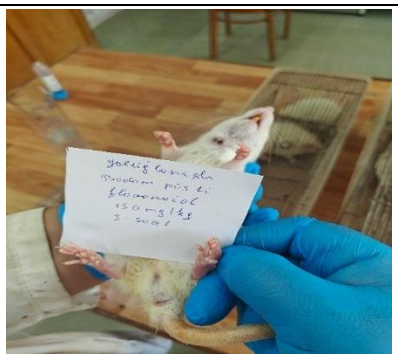	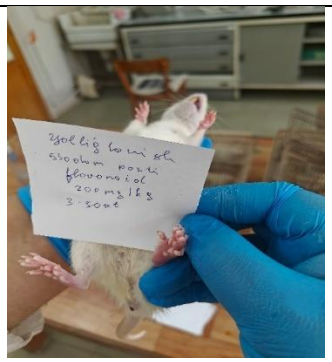
Almond steam bark-Flavanoid 150 mg/kg	Almond steam bark-Flavanoid 150 mg/kg
	
Almond steam bark-Rutin 25 mg/kg	Almond steam bark-Rutin 50 mg/kg
	
Almond steam bark-Rutin 75 mg/kg	

Taken together, the results from this model provide compelling evidence that both rutin and the flavonoid-rich fraction isolated from almond steam bark possess substantial anti-inflammatory activity. Their ability to significantly suppress carrageenan-induced edema formation in vivo, particularly at relatively low doses, supports their pharmacological potential as natural therapeutic agents. These findings warrant further investigation into their mechanisms of action, chronic inflammation models, and eventual clinical applicability.

Molecular docking results

To better understand the molecular basis of the anti-inflammatory and pharmacological potential of rutin, we conducted a series of molecular docking simulations with key protein targets involved in inflammation, apoptosis, signal transduction, and drug transport. These targets included tumor necrosis factor-alpha (TNF-α), AKT serine/threonine kinase 1 (AKT1), B-cell lymphoma 2 (BCL2), serum albumin (ALB), and estrogen receptor 1 (ESR1). Each of these proteins plays a distinct and crucial role in pathophysiological processes such as chronic inflammation, cancer progression, and metabolic dysregulation.

Docking studies were performed using the AutoDock software to evaluate rutin's ability to bind to the active sites of these targets. Binding energies (ΔG), inhibition constants (Ki), and interaction profiles including hydrogen bonding, hydrophobic contacts, and electrostatic interactions were calculated. The results provide insight into the potential of rutin as a bioactive compound capable of modulating molecular pathways through direct protein–ligand interactions.

The following subsections describe in detail the binding affinity and interaction patterns between rutin and each selected protein target.

Tumor necrosis factor-alpha

Tumor necrosis factor-alpha (TNF-α, PDB ID: 2AZ5) is one of the key cytokines responsible for activating immune responses and regulating inflammatory processes. This protein plays an essential role in the body's defense mechanisms, including the destruction of neoplastic cells, apoptosis, inflammation, and protection against infections. However, excessive activity of TNF-α contributes significantly to the development of chronic pathological conditions such as rheumatoid arthritis, inflammatory bowel disease, psoriasis, neurodegenerative disorders, and diabetes. Therefore, compounds that inhibit TNF-α are of considerable therapeutic interest.

In our *in silico* experiment, the flavonoid rutin was docked with the TNF-α protein using the AutoDock software. Molecular docking results showed that rutin binds to the active site of TNF-α at the coordinates X = −18.335, Y = 64.771, Z = 26.730, releasing a binding energy of −7.8 kcal/mol. This negative binding energy indicates a spontaneous interaction between the flavonoid and the protein, occurring without external energy input. Based on this energy value, the inhibition constant (Ki) was calculated. At ΔG = −7.8 kcal/mol, the Ki was determined to be 1.92 μM, indicating a strong binding affinity (**Figure 5**).

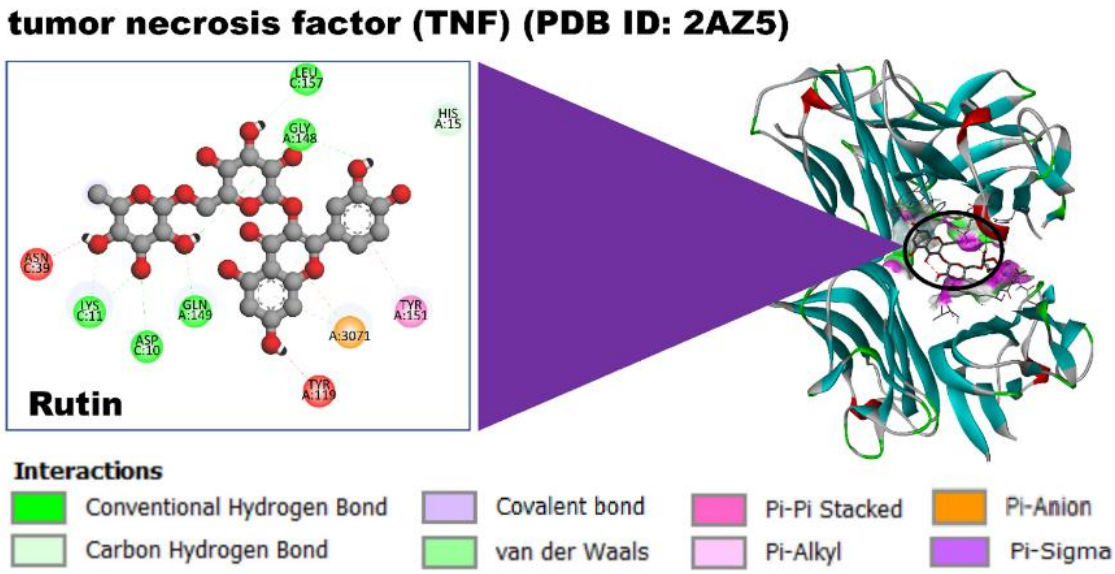

Figure 5 Molecular docking model of rutin bound to tumor necrosis factor-alpha (TNF-α, PDB ID: 2AZ5). On the right, the 3-dimensional structure of the TNF-α protein is shown, with the rutin molecule located within the active binding pocket (highlighted by a black circle). On the left, the interaction diagram illustrates the key molecular contacts between rutin and amino acid residues of TNF-α. Conventional hydrogen bonds were observed with GLY A:148, ASP C:10, LYS C:11, GLN A:149, and LEU C:157. Additional interactions included pi-anion, pi-pi stacked, and hydrogen bonds involving ASN C:39, TYR A:119, and TYR A:151. These interactions collectively contribute to the stable binding of rutin within the TNF-α active site.

Rutin interacted with several amino acid residues of the TNF-α protein, including ASN C:39, LYS C:11, ASP C:10, GLN A:149, TYR A:119, TYR A:151, HIS A:15, LEU C:157, and GLY A:148, forming conventional and carbon hydrogen bonds, as well as unfavorable donor-donor, pi-cation, and pi-pi stacked interactions. Amino acids such as ASN, GLN, ASP, and GLY tend to form hydrogen bonds and contribute to specific ligand-protein interactions. LYS and HIS residues can establish pi-cation bonds through their aromatic or charged side chains, while TYR residues, due to their phenolic structure, participate in pi-pi stacking interactions. LEU contributes to hydrophobic interactions, enhancing structural stability.

The binding of rutin to TNF-α through these residues effectively blocks the protein's active site, potentially disrupting its role in inflammatory signal transduction. Inhibiting TNF-α in this manner may represent a promising therapeutic strategy for managing inflammation and autoimmune diseases associated with its overproduction. Therefore, rutin is evaluated as a potential natural and effective TNF-α inhibitor.

AKT serine/threonine kinase 1 (AKT1)

AKT serine/threonine kinase 1 (AKT1, PDB ID: 7NH5) is a central component of intracellular signal transduction cascades and plays a key regulatory role in cell growth, proliferation, metabolism, and survival through the PI3K/AKT/mTOR pathway. Activation of AKT1 occurs via phosphorylation in response to various receptor stimulations and is involved in vital biological processes such as proliferation, anti-apoptosis, angiogenesis, and glucose metabolism. However, hyperactivation or constitutive activity of AKT1 is closely associated with the development of numerous cancers, insulin resistance, cardiovascular diseases, and neurodegenerative disorders, making it a valuable therapeutic target (**Figure 6**).

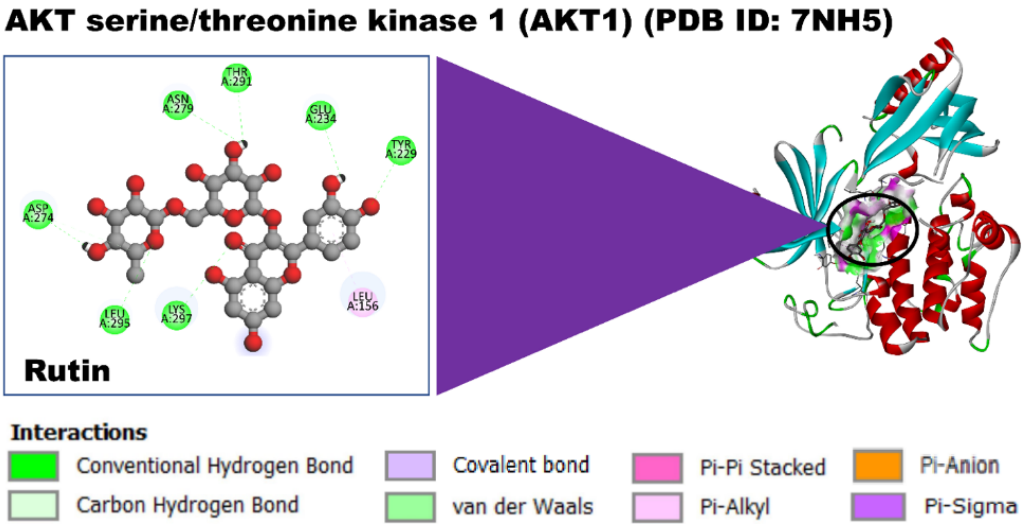

Figure 6. Binding model of the rutin molecule with AKT1 kinase (PDB ID: 7NH5). Rutin interacts with AKT1 through multiple hydrogen bonds involving amino acid residues such as TYR A:229, THR A:291, GLU A:234, ASP A:274, and others.

In our subsequent *in silico* experiment, the flavonoid rutin was docked with the AKT1 protein using AutoDock software. According to the molecular docking results, rutin binds to the central active site of AKT1 at the coordinates X = 9.145000, Y = −13.570000, Z = −17.714000, forming a stable complex with a binding energy of −8.8 kcal/mol. This negative energy indicates that the interaction occurs spontaneously and is thermodynamically favorable. Based on the binding energy (ΔG = −8.8 kcal/mol = −36,800 J/mol), the inhibition constant (Ki) was calculated using the equation $Ki = e^{(\Delta G \times 1{,}000/RT)}$, yielding:

$$Ki \approx e^{(-36800/(8.314\times298))} \approx e^{(-14.84)} \approx 3.6\times10^{-7}\ M = 0.36\ \mu M.$$

This result suggests that rutin binds to AKT1 with submicromolar affinity, indicating a very strong interaction. Rutin formed conventional and carbon hydrogen bonds, as well as pi-alkyl interactions with several amino acid residues of AKT1, including ASP A:274, LEU A:295, LYS A:297, LEU A:156, TYR A:229, GLU A:234, THR A:291, and ASN A:279. Amino acids such as ASP, GLU, and ASN exhibit hydrophilic properties, facilitating the formation of hydrogen bonds. LYS, being a positively charged residue, contributes to hydrogen bonding and ionic interactions. LEU and TYR, with their hydrophobic and aromatic nature, are involved in pi–alkyl and van der Waals interactions.

These residues are likely located in the ATP-binding site or functionally important phosphorylation-related domains of AKT1, suggesting that rutin may block the catalytic activity of the protein. The inhibition of AKT1 by rutin could therefore serve as a critical therapeutic strategy to suppress pathological conditions arising from AKT1 overactivation, particularly cancer and metabolic syndromes.

Consequently, rutin is proposed as a promising natural inhibitor of AKT1, capable of modulating intracellular signaling pathways by suppressing cell growth and survival mechanisms through direct interaction with the protein's active site.

B-cell lymphoma 2 (BCL2)

B-cell lymphoma 2 (BCL2, PDB ID: 6GL8) is a key anti-apoptotic protein localized in the mitochondrial membranes, where it plays a central role in regulating programmed cell death (apoptosis). As a member of the BCL2 protein family, it protects cells from apoptotic stimuli and prolongs cell survival by regulating mitochondrial membrane permeability, inhibiting the release of cytochrome c, and preventing the activation of caspases. Due to these protective functions, BCL2 is often overexpressed in various cancer cells, which contributes to their resistance to apoptosis and reduced sensitivity to chemotherapy. Consequently, the discovery of BCL2 inhibitors is considered a promising strategy in cancer therapy.

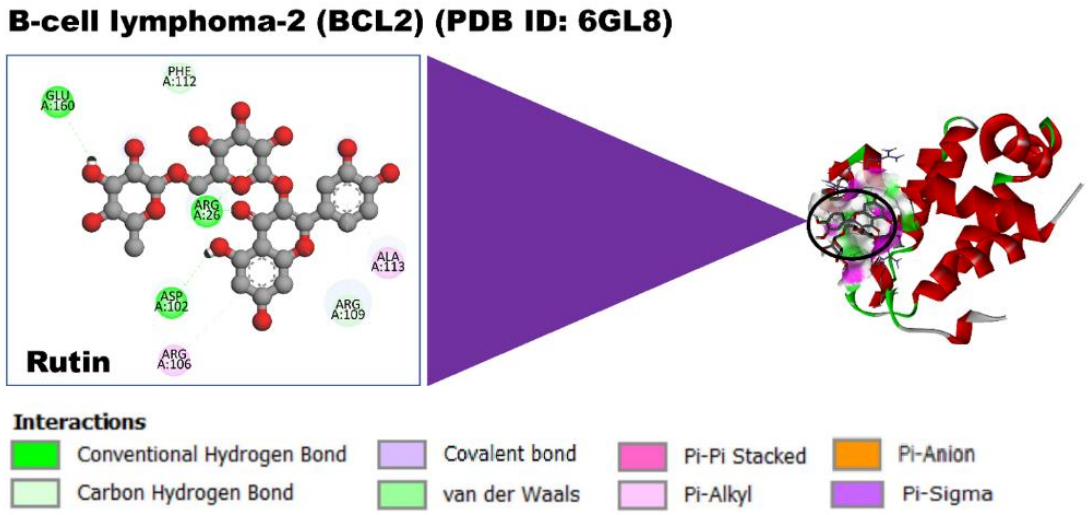

Figure 7 Binding diagram of the rutin molecule with B-cell lymphoma-2 (BCL2, PDB ID: 6GL8). Rutin interacts with amino acid residues GLU A:160, ASP A:102, ARG A:26, and PHE A:112 through conventional hydrogen bonds, carbon hydrogen bonds, and pi–alkyl interactions. The 3-dimensional structure of the protein is shown on the right, while the binding site is illustrated on the left.

In our *in silico* study, the flavonoid rutin was docked with the BCL2 protein using AutoDock software. Docking results showed that rutin binds to the active site of BCL2 located at the coordinates X = −5.006000, Y = −6.075000, Z = 6.349000, forming a stable complex with a binding energy of −6.8 kcal/mol. This negative value indicates that the interaction is spontaneous and thermodynamically favorable. The estimated inhibition constant (Ki) was calculated to be 10.6 μM, suggesting a moderate binding affinity at the micromolar level.

Rutin was found to interact with several amino acid residues in BCL2, including ASP A:102, ARG A:106, ARG A:109, ARG A:26, ALA A:109, PHE A:112, and GLU A:160, forming conventional hydrogen bonds, carbon hydrogen bonds, and pi-alkyl interactions. Acidic residues such as ASP and GLU are actively involved in hydrogen bond formation. ARG, with its guanidinium group, provides a charged environment rich in hydrogen bonding potential. ALA, with its small hydrophobic side chain, contributes to structural stability, while PHE, due to its aromatic structure, participates in pi-alkyl interactions (**Figure 7**).

These residues are likely located within or near the BH (BCL2 homology) domains or other functional regions of the protein. By binding to these sites, rutin may disrupt the anti-apoptotic function of BCL2. As a result, rutin is proposed to act as a promising natural inhibitor of BCL2, capable of weakening its protective effect and promoting apoptosis in cancer cells.

Serum albumin (ALB)

Serum albumin (ALB, PDB ID: 6R7S) is the most abundant plasma protein in the human body, primarily synthesized in the liver, and plays a crucial role as a transporter in the bloodstream. ALB facilitates the transport of water-insoluble or poorly soluble molecules - particularly free fatty acids, hormones, drugs, polyphenols, and other hydrophobic compounds - throughout the body. Additionally, albumin is essential for maintaining plasma osmotic pressure, providing antioxidant defense, and acting as a pH buffer. It also significantly influences the pharmacokinetics of many therapeutic agents, including their tissue distribution, half-life, and clearance rates. Therefore, studying the interaction of bioactive compounds with ALB is important not only for pharmacodynamics but also for pharmacokinetics.

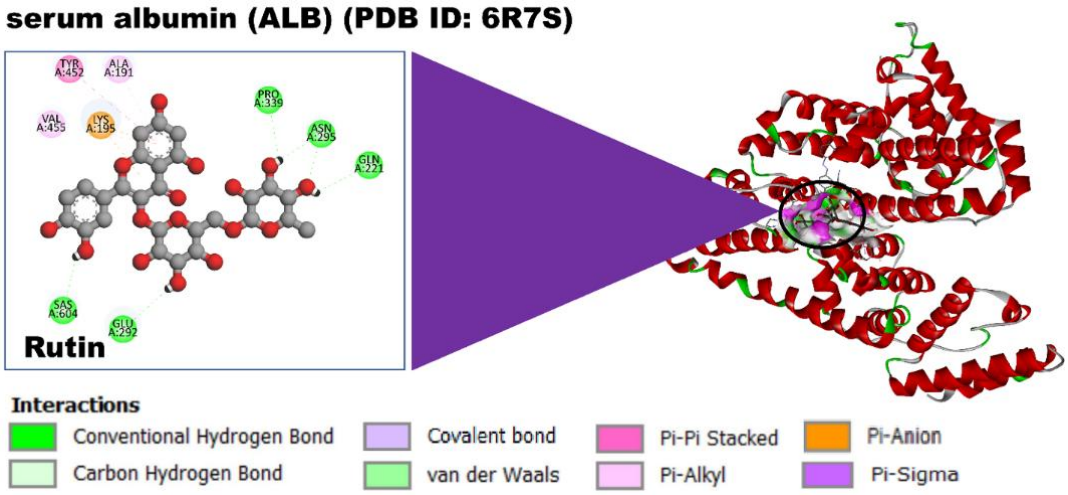

Figure 8 Binding model of the rutin molecule with serum albumin (ALB, PDB ID: 6R7S). Rutin interacts with amino acid residues such as GLU A:292, ASN A:295, PRO A:339, TYR A:452, and others through hydrogen bonds, pi-anion interactions, and van der Waals forces.

In our *in silico* experiment, the flavonoid rutin was docked with the ALB protein using AutoDock software. The docking results showed that rutin binds to the active site of ALB, located at coordinates X = 4.390000, Y = 5.227000, Z = 17.396000, forming a stable complex with a binding energy of -10.4 kcal/mol. This negative energy indicates a thermodynamically favorable and spontaneous interaction. Based on this value, the inhibition constant (Ki) was calculated to be 23.2 nM, suggesting that rutin binds to ALB with high affinity at the nanomolar level.

The binding involved several amino acid residues, including VAL A:455, TYR A:452, ALA A:191, LYS A:195, PRO A:339, ASN A:295, GLN A:221, GLU A:292, and SAS A:604. Rutin formed conventional hydrogen bonds, carbon hydrogen bonds, and pi-alkyl interactions with these residues. Hydrophobic amino acids such as VAL, ALA, and PRO may contribute to van der Waals or pi-alkyl interactions with the phenolic and alkyl portions of the flavonoid. The aromatic ring of TYR can participate in pi-pi or pi-alkyl interactions, while charged residues LYS and GLU are capable of forming ionic and hydrogen bonds. Polar residues ASN and GLN are likely to interact with the hydrophilic groups of rutin through hydrogen bonding (**Figure 8**).

These amino acids are located in potential ligand-binding regions of ALB, and the occupation of these sites by rutin may temporarily interfere with the protein's transport function. By binding strongly to ALB, rutin may influence its own pharmacokinetic profile, possibly leading to extended circulation time, slower tissue distribution, and delayed elimination. Therefore, the strong and selective binding of rutin to ALB plays a key role in determining how this compound circulates and exerts its effects within the body. Such interactions are critical for evaluating the therapeutic form, dosing regimen, and potential side effects of natural compounds that exhibit high binding affinity to albumin. In this context, rutin is recognized as a promising bioactive flavonoid with strong binding capacity to ALB.

Estrogen receptor 1 (ESR1)

Estrogen receptor 1 (ESR1, PDB ID: 1L2I) is a transcriptional activator protein belonging to the nuclear receptor superfamily. It binds to estrogen hormones and regulates gene expression within cells. ESR1 activity plays a crucial role not only in sexual development and reproductive processes but also in various biological conditions associated with inflammation. Research indicates that ESR1 can modulate the expression of key inflammatory mediators such as IL-6, TNF-α, and COX-2, making it a significant factor in the pathophysiology of chronic inflammatory diseases, including cardiovascular disorders, metabolic syndrome, osteoarthritis, and autoimmune conditions.

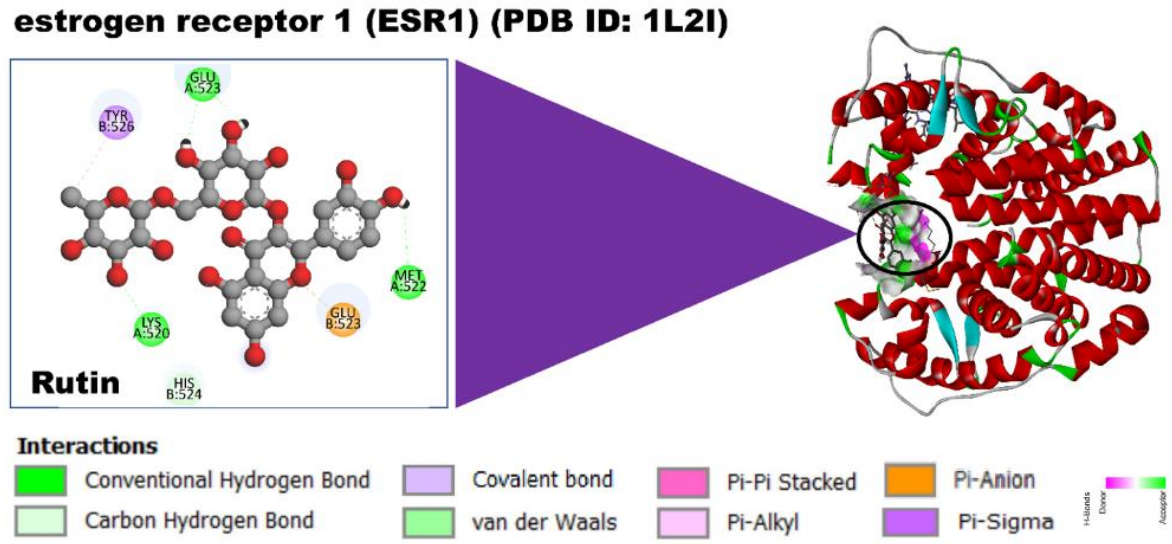

Figure 9 Binding model of the rutin molecule with estrogen receptor 1 (ESR1, PDB ID: 1L2I). The 3-dimensional structure of the ESR1 protein is shown on the right, with the rutin molecule positioned in the active binding site (highlighted with a black circle). On the left, detailed molecular interactions between rutin and amino acid residues are illustrated. Rutin interacts with GLU A:523, LYS A:520, MET A:522, TYR B:526, HIS B:524, and GLU B:523 through conventional hydrogen bonds, carbon hydrogen bonds, and pi-anion interactions. The types of interactive forces are represented in various colors as indicated in the legend below the diagram.

Thus, the identification of natural compounds capable of regulating ESR1 activity represents a promising strategy for controlling inflammation-related processes. In our *in silico* study, the flavonoid rutin was docked with the ESR1 protein using the molecular docking tool AutoDock. According to the docking results, rutin binds to the active site of ESR1 with a binding energy of −8.5 kcal/mol, forming a stable complex. This negative energy indicates that the interaction is spontaneous and thermodynamically favorable.

At $\Delta G = -8.5$ kcal/mol = −35,566 J/mol, the inhibition constant (Ki) was calculated as follows:

$$Ki \approx e^{(-35{,}566/(8.314\times298))} \approx e^{(-14.31)} \approx 6.1\times10^{-7}\ M = 0.61\ \mu M.$$

This result demonstrates that rutin binds to ESR1 with strong and selective affinity at the micromolar level. The interaction occurred through several amino acid residues of ESR1, including LYS A:520, HIS B:524, GLU B:523, MET A:522, GLU A:523, and TYR B:526. These interactions involved conventional hydrogen bonds, carbon hydrogen bonds, pi-anion, and pi-cation interactions. Charged residues such as LYS and HIS formed pi-cation interactions, enhancing the electrostatic affinity with the aromatic rings of rutin. GLU, with its negatively charged side chain, participated in pi-anion interactions. Hydrophobic and aromatic residues MET and TYR were involved in pi interactions or van der Waals forces (**Figure 9**).

These residues are likely located near ESR1's estrogen-binding domain or transcriptional activation regions, implying that rutin may modulate ESR1 activity by occupying these functional sites. The strong and selective interaction between rutin and ESR1 suggests the potential of rutin to indirectly suppress inflammation-related signaling pathways such as NF-κB or JAK/STAT.

Overactivation of ESR1 may lead to excessive expression of pro-inflammatory genes. By limiting ESR1 activity, rutin could reduce the production of inflammatory mediators. This supports its potential as a natural anti-inflammatory agent with therapeutic relevance. Therefore, rutin is considered a promising bioactive compound capable of mitigating or regulating chronic inflammatory conditions through its interaction with ESR1.

Discussion

The present study provides a comprehensive investigation into the extraction, purification, safety, anti-inflammatory activity, and molecular interaction profile of flavonoid and rutin compounds derived from Prunus amygdalus (almond) steam bark. The sequential ethanol-based extraction combined with ultrasonic treatment and vacuum concentration yielded a high-purity (98.0 ± 0.8%) total flavonoid fraction, while semi-preparative HPLC allowed for the efficient isolation of rutin with high chromatographic resolution. These results underscore the efficiency of the applied extraction-purification workflow, which preserved the integrity of thermolabile polyphenolic structures and minimized potential oxidative degradation during processing.

The acute oral toxicity evaluation revealed that both the flavonoid fraction and purified rutin exhibited minimal transient behavioral alterations at the highest tested dose of 5,000 mg/kg, with no mortality or body weight changes over 14 days. This observation aligns with previous reports indicating that flavonoids generally have low acute toxicity profiles, even at gram-per-kilogram dosing levels, which supports their classification under GHS Category 5 (low toxicity). The absence of gastrointestinal distress, tremors, or neurological symptoms further suggests favorable systemic tolerance, providing a solid safety foundation for future pharmacological applications.

In the carrageenan-induced paw edema model, both compounds demonstrated marked anti-inflammatory activity, with lower doses showing comparatively greater inhibition of edema formation than higher doses. This inverted dose-response effect could be attributed to factors such as enhanced bioavailability at lower concentrations, reduced aggregation in biological fluids, and avoidance of receptor saturation. Flavonoids at 100 mg/kg and rutin at 25 mg/kg yielded the highest inhibition rates (61.6% and 55.6%, respectively) during the prostaglandin-dominated phase of inflammation. This supports the hypothesis that these compounds may act through cyclooxygenase (COX) modulation, as well as via suppression of pro-inflammatory cytokines such as TNF-α and IL-6.

The sustained but gradually declining inhibition observed in later hours post-carrageenan injection likely reflects metabolic clearance and redistribution of the compounds. Nevertheless, statistically significant inhibition persisted throughout the experiment, indicating prolonged biological activity. These in vivo results complement earlier antioxidant findings, suggesting that the observed anti-inflammatory activity is mediated by both direct inhibition of inflammatory signaling and indirect cytoprotective effects via reactive oxygen species (ROS) scavenging.

Molecular docking studies provided a mechanistic basis for the *in vivo* observations. Rutin demonstrated strong binding affinities to several key protein targets involved in inflammation and cell survival pathways, including TNF-α (-7.8 kcal/mol, Ki = 1.92 μM), AKT1 (−8.8 kcal/mol, Ki = 0.36 μM), and ESR1 (−8.5 kcal/mol, Ki = 0.61 μM), as well as high-affinity binding to serum albumin (−10.4 kcal/mol, Ki = 23.2 nM). The interactions involved hydrogen bonding, hydrophobic contacts, and π–π stacking, with amino acid residues localized in functionally important regions of the target proteins.

The inhibition of TNF-α and AKT1 may explain the suppression of pro-inflammatory cytokine production and downstream inflammatory cascades, while ESR1 modulation could contribute to regulation of NF-κB-mediated transcription of inflammatory mediators. The strong binding to serum albumin suggests a prolonged plasma half-life, potentially enhancing systemic exposure and therapeutic effect duration. Notably, rutin's interaction with BCL2 (−6.8 kcal/mol, Ki = 10.6 μM) indicates a moderate ability to influence apoptotic pathways, which could be relevant in chronic inflammatory diseases where dysregulated cell survival plays a role.

Taken together, the combined in vivo and in silico evidence strongly supports the pharmacological potential of almond steam bark-derived flavonoids and rutin as natural anti-inflammatory agents with low acute toxicity. The concordance between molecular docking predictions and experimental results enhances confidence in their mechanistic plausibility.

Conclusions

This study successfully optimized the extraction and purification of high-purity flavonoids and rutin from *Prunus amygdalus* steam bark, confirmed their safety in acute oral toxicity testing, and demonstrated significant

anti-inflammatory activity in a carrageenan-induced paw edema model. The observed biological effects were supported by molecular docking analyses, which revealed strong interactions of rutin with multiple inflammation-related protein targets, suggesting multi-targeted modulation of inflammatory and survival pathways. The combination of low acute toxicity, potent anti-inflammatory effects, and favorable binding profiles positions almond steam bark-derived flavonoids and rutin as promising candidates for development into pharmacological formulations, functional foods, or nutraceuticals. Future research should focus on subacute and chronic toxicity studies, pharmacokinetic profiling, and clinical validation to further elucidate their therapeutic potential and optimize dosing strategies.

Acknowledgement

This study is carried out by Lazizbek Makhmudov we would like to thank Institute of Bioorganic Chemistry named after A. S. Sadykov.

Declaration of Generative AI in Scientific Writing

Only minimal assistance was used from QuillBot for paraphrasing selected sentences. All scientific content, interpretation, and conclusions were developed independently by the authors.

References

[1] I Garrido, M Monagas, C Gómez-Cordovés and B Bartolomé. Almond (*Prunus dulcis* (Mill.) D.A. Webb) skins as a potential source of bioactive polyphenols. *Journal of Agricultural and Food Chemistry* 2007; **56(23)**, 10198-10205

[2] T Ben Khadher, S Sassi-Aydi, S Aydi, M Mars and J Bouajila. Phytochemical profiling and biological potential of *Prunus dulcis* shell extracts. *Plants* 2023; **12(14)**, 2733.

[3] G Ulugbek, A Izzatullo, S Fotima, O Sirojiddin, A Azizbek, G Sabina and T Aripov. Plant derived and synthetical antihypoxic agents in cardiovascular diseases: Mechanisms, key pathways and therapeutic potential. *Plant Science Today* 2025; **12(4)**, 1-10.

[4] N Dhingra, A Kar, R Sharma and S Bhasin. *In-vitro* antioxidative potential of different fractions from *Prunus dulcis* seed extract. *Industrial Crops and Products* 2017; **74**, 427-433.

[5] S Yada, K Lapsley and G Huang. A review of the composition and health benefits of almonds. *Journal of Food Science* 2011; **76(9)**, C773-C783.

[6] I Abdullaev, U Gayibov, S Omonturdiev, S Fotima, S Gayibova and T Aripov. Molecular pathways in cardiovascular disease under hypoxia: Mechanisms, biomarkers, and therapeutic target. *The Journal of Biomedical Research* 2025; **39(3)**, 254-269.

[7] A Abdullaev, I Abdullaev, A Bogbekov, U Gayibov, S Omonturdiev, S Gayibova, M Turahodjayev, K Ruziboev and T Aripov. Antioxidant potential of *Rhodiola heterodonta* extract: Activation of Nrf2 pathway via integrative *in vivo* and *in silico* studies. *Trends in Sciences* 2025; **22(5)**, 9521.

[8] S Sodiqova, S Kadirova, A Zaynabiddinov, I Abdullaev, L Makhmudov, U Gayibov, M Yuldasheva, M Xolmirzayeva, R Rakhimov, A Mutalibov and H Karimjonov. Channelopathy activity of a-41(propyl ester of gallic acid): Experimental and computational study of antihypertensive activity. *Trends in Sciences* 2025; **22(9)**, 10496.

[9] AB Enogieru, W Haylett, DC Hiss, S Bardien and OE Ekpo. Rutin as a potent antioxidant: Implications for neurodegenerative disorders. *Oxidative Medicine and Cellular Longevity* 2018; **2018(1)**, 6241017.

[10] PAV Freitas, L Martín-Pérez, I Gil-Guillén, C González-Martínez and A Chiralt. Subcritical water extraction for valorisation of almond skin from almond industrial processing. *Foods* 2023; **12(20)**, 3759.

[11] D Barreca, SM Nabavi, A Sureda, M Rasekhian, R Raciti, AS Silva, G Annunziata, A Arnone, GC Tenore, I Süntar and G Mandalari. Almonds (*Prunus dulcis* Mill. D. A. Webb): A source of nutrients and health-promoting compounds. *Nutrients* 2020; **12(3)**, 672.

[12] JO Chaves, MCA De Souza, LC Da Silva, D Lachos-Perez, PC Torres-Mayanga, APDF Machado, T Forster-Carneiro, M Vázquez-Espinosa, AV González-de-Peredo, GF Barbero and MA Rostagno. Extraction of flavonoids from natural sources using modern

techniques. *Frontiers in Chemistry* 2020; **25(8)**, 507887.

[13] SE Bianchi, S Kaiser, V Pittol, E Doneda, KCB De Souza and VL Bassani. Semi-preparative isolation and purification of phenolic compounds from *Achyrocline satureioides* (Lam) D.C. by high-performance counter-current chromatography. *Phytochemical Analysis* 2018; **30(2)**, 182-192.

[14] O Gaibullayeva, A Islomov, D Abdugafurova, B Elmurodov, B Mirsalixov, L Mahmudov, I Adullaev, K Baratov, S Omonturdiev and S Sa'dullayeva. *Inula helenium* L. root extract in sunflower oil: Determination of its content of water-soluble vitamins and immunity-promoting effect. *Biomedical and Pharmacology Journal* 2024; **17(4)**, 2729-2737.

[15] I Abdurazakova, A Zaynabiddinov, I Abdullaev, L Makhmudov, U Gayibov, S Omonturdiev, G Abdullayev, M Xolmirzayeva and S Zhurakulov. Pharmacological Evaluation of F45 on the Cardiovascular System using *In Vitro*, *In Vivo* Models and Molecular Dockings. *Trends in Sciences* 2025; **22(12)**, 10924.

[16] A Khasanov, I Abdullaev, S Kadirova, M Mamajanov, A Zaynabiddinov, S Omonturdiev, L Makhmudov, D Inomjonov, U Gayibov, R Esanov and A Matchanov. N-2 Polyphenol Targets Vascular Calcium Channels to Exert Antihypertensive Effects: *In Vitro* and *In Vivo* Evaluation. *Trends in Sciences* 2025; **22(12)**, 10782.

[17] R Sayidaliyeva, S Kadirova, A Zaynabiddinov, I Abdullaev, L Makhmudov, U Gayibov, M Yuldasheva, M Kholmirzayeva, R Rakhimov, A Mutalibov and H Karimjonov. A-51 as A Natural Calcium Channel Blocker: An Integrative Study Targeting Hypertension. *Trends in Sciences* 2025; **22(11)**, 10760.

[18] MT Mansouri, AA Hemmati, B Naghizadeh, SA Mard, A Rezaie and B Ghorbanzadeh. A study of the mechanisms underlying the anti-inflammatory effect of ellagic acid in carrageenan-induced paw edema in rats. *Indian Journal of Pharmacology* 2015; **47(3)**, 292-298.

[19] S Amdekar, P Roy, V Singh, A Kumar, R Singh and P Sharma. Anti-inflammatory activity of lactobacillus on carrageenan-induced paw edema in male wistar rats. *International Journal of Inflammation* 2012; **2012**, 752015.

[20] M Zaripova, I Abdullaev, A Bogbekov, U Gayibov, S Omonturdiev, R Makhmudov, N Ergashev, G Jabbarova, S Gayibova and T Aripov. *In vitro* and *in silico* studies of Gnaphalium U. extract: Inhibition of α-amylase and α-glucosidase as a potential strategy for metabolic syndrome regulation. *Trends in Sciences* 2025; **22(8)**, 10098.

[21] XY Meng, HX Zhang, M Mezei and M Cui. Molecular docking: A powerful approach for structure-based drug discovery. *Current Computer-Aided Drug Design* 2011; **7(2)**, 146-157.

[22] EC Aytar, EI Torunoglu, A Gümrükçüoğlu, A Durmaz, S Al-Farraj and M Sillanpää. Molecular docking analyses on the chemical profile and antioxidant potential of Cakile maritima using GC-MS and HPLC. *Scientific Reports* 2025; **15(1)**, 1-22.

[23] MV Alvarez, S Cabred, CL Ramirez and MA Fanovich. Fluids valorization of an agroindustrial soybean residue by supercritical fluid extraction of phytochemical compounds. *The Journal of Supercritical Fluids* 2019; **143**, 90-96.

[24] M Bimakr, RA Rahman, FS Taip, A Ganjloo, L Salleh, J Selamat, A Hamid and ISM Zaidul. Comparison of different extraction methods for the extraction of major bioactive flavonoid compounds from spearmint (*Mentha spicata* L.) leaves. *Food and Bioproducts Processing* 2011; **89(1)**, 67-72.

[25] I Susanti, R Pratiwi, Y Rosandi and AN Hasanah. Separation methods of phenolic compounds from plant extract as antioxidant agents candidate. *Plants* 2024; **13(7)**, 965.

[26] T Ben Khadher, S Sassi-Aydi, S Aydi, M Mars and J Bouajila. Phytochemical profiling and biological potential of *Prunus dulcis* shell extracts. *Plants* 2023; **12(14)**, 2733.

[27] S Sang, K Lapsley, WS Jeong, PA Lachance, CT Ho and RT Rosen. Antioxidative phenolic compounds isolated from almond skins (*Prunus amygdalus* Batsch). *Journal of Agricultural and Food Chemistry* 2002; **50(8)**, 2459-2463.

[28] Toxicological Profile for Endosulfan. *Public health statement for endosulfan*. Agency for Toxic

Substances and Disease Registry, Atlanta, Georgia, 2015.

[29] L Wang, Z Guo, D Cui, S Ul Haq, W Guo, F Yang and H Zhang. Toxicological evaluation of the ultrasonic extract from *Dichroae radix* in mice and wistar rats. *Scientific Reports* 2020; **10**, 18206.

[30] MP Motwani, JD Flint, RPH De Maeyer, JN Fullerton, AM Smith, DJB Marks and DW Gilroy. Novel translational model of resolving inflammation triggered by UV-killed *E. coli*. *The Journal of Pathology: Clinical Research* 2016; **2(3)**, 154-165.

[31] Y Du, Y Dou, M Wang, Y Wang, Y Yan, H Fan, N Fan, X Yang and X Ma. Efficacy and acceptability of anti-inflammatory agents in major depressive disorder: A systematic review and meta-analysis. *Frontiers in Psychiatry* 2024; **15**, 1407529.

[32] AQQ Azimova, AX Islomov, SA Maulyanov, DG Abdugafurova, LU Mahmudov, IZ Abdullaev, AS Ishmuratova, SQ Siddikova and IR Askarov. Determination of vitamins and pharmacological properties of *Vitis vinifera* L. plant fruit part (mixed varieties) syrup-honey. *Biomedical and Pharmacology Journal* 2024; **17(4)**, 2779-2786.

[33] M Mamajanov, I Abdullaev, G Sotimov, S Mavlanova, Q Niyozov, M Mirzaolimov, A Najimov, E Mirzaolimov, M Raximberganov and U Abdullayev. Mitochondrial and Pharmacokinetic Insights into 3,5,7,2’,6’-Pentahydroxyflavanone: Respiratory Modulation, Calcium Handling, and Membrane Stability. *Trends in Sciences* 2025; **22(12)**, 10984.

[34] AG Vakhobjonovna, KE Jurayevich, AIZ Ogli, EN Azamovich, MR Rasuljonovich and AM Islomovich. Tannins as modulators in the prevention of mitochondrial dysfunction. *Trends in Sciences* 2025; **22(8)**, 10436.